Study of time reversibility/irreversibility of cardiovascular data: theoretical results and application to laser Doppler flowmetry and heart rate variability signals

Anne Humeau-Heurtier[1]**, Guillaume Mahé**[2]**,
François Chapeau-Blondeau**[1]**, David Rousseau**[3] **and Pierre Abraham**[2]

[1] LUNAM Université, Université d'Angers, LISA—Laboratoire d'Ingénierie des Systèmes Automatisés, 62 avenue Notre Dame du Lac, 49000 Angers, France
[2] LUNAM Université, Angers France, Université d'Angers, CHU Angers, Laboratoire de Physiologie et d'Explorations Vasculaires, UMR CNRS 6214-INSERM 1083, 49933 Angers cedex 09, France
[3] Université de Lyon, CREATIS, CNRS UMR5220, INSERM U630, Université de Lyon 1, INSA-Lyon, 69621 Villeurbanne, France

E-mail: anne.humeau@univ-angers.fr

Abstract

Time irreversibility can be qualitatively defined as the degree of a signal for temporal asymmetry. Recently, a time irreversibility characterization method based on entropies of positive and negative increments has been proposed for experimental signals and applied to heart rate variability (HRV) data (*central* cardiovascular system (CVS)). The results led to interesting information as a time asymmetry index was found different for young subjects and elderly people or heart disease patients. Nevertheless, similar analyses have not yet been conducted on laser Doppler flowmetry (LDF) signals (peripheral CVS). We first propose to further investigate the above-mentioned characterization method. Then, LDF signals, LDF signals reduced to samples acquired during ECG R peaks (LDF_R_{ECG} signals) and HRV recorded simultaneously in healthy subjects are processed. Entropies of positive and negative increments for LDF signals show a nonmonotonic pattern: oscillations—more or less pronounced, depending on subjects—are found with a period matching the one of cardiac activity. However, such oscillations are not found with LDF_R_{ECG} nor with HRV. Moreover, the asymmetry index for LDF is markedly different from the ones of LDF_R_{ECG} and HRV. The cardiac activity may therefore play a dominant role in the time irreversibility properties of LDF signals.

(Some figures may appear in colour only in the online journal)

1. Introduction

When studying the cardiovascular system (CVS), two viewpoints can be adopted: a central viewpoint and a peripheral viewpoint. A central viewpoint is given by the analysis of data reflecting the activities at the heart itself. Electrocardiogram (ECG) and heart rate variability (HRV) are such kinds of data. A peripheral viewpoint of the CVS can be given by laser Doppler flowmetry (LDF) signals. The LDF technique relies on the interaction of laser photons and moving blood cells (see for example Humeau *et al* 2007b). When laser photons encounter moving blood particles, their wavelength is changed according to the Doppler effect. The backscattered photons are collected (very often by an optical fiber) and led to a signal processing unit. The first moment of the photocurrent power spectrum gives the LDF signal that reflects the microvascular perfusion. LDF data are now commonly used in clinical research to monitor microvascular blood flow and are the subject of many papers (see for example Bernjak *et al* 2011, Tew *et al* 2011, Wojtkiewicz *et al* 2011, Binzoni *et al* 2010, 2009, Okano *et al* 2010, Al-Tahami *et al* 2010).

Numerous biophysical processes play a role in the CVS. Each of them has its own characteristic time scales and all of them interplay together. The CVS therefore presents complex behaviors. Many analyses have been performed on time series from the CVS (see for example Signorini *et al* 2011, Costa *et al* 2008, 2005, Ivanov *et al* 1999). Their goal was to better understand the CVS or the data themselves, or for diagnosis purposes. Thus, the study of the time reversibility/irreversibility properties has been applied to HRV data (Costa *et al* 2008, 2005) and also very recently to fetal magnetocardiographic recordings (Hoyer *et al* 2012). A signal can be qualitatively considered as time reversible if its statistical properties are invariant with respect to time reversal. The practical approach to irreversibility proposed by Costa *et al* can be based on a notion of entropy for the fluctuation. This method of Costa *et al* for a characterization of time irreversibility led to interesting applications with a time asymmetry index which was found to be higher in HRV from young subjects and to decrease with aging or heart disease (Costa *et al* 2005). These results can be of importance for the development and tests of physiological models. Nevertheless, from the best of our knowledge, time irreversibility/reversibility has not yet been studied for data from the peripheral CVS such as LDF signals.

In Costa *et al* (2005), the method for a characterization of time irreversibility was defined, and then it was directly applied to the analysis of HRV. As a complement, we first propose herein a theoretical analysis of the properties of this approach in order to better appreciate its capabilities, expected behaviors and limitations. To this purpose, the characterization method is applied to several kinds of random signal models of known temporal constitution. In each case, the theoretical behavior of the method is derived and studied analytically. Then, the characterization method is applied to LDF signals, to LDF signals reduced to samples acquired during ECG R peaks (LDF_R_{ECG} signals) and to HRV recorded simultaneously.

The purpose of our work is therefore threefold: (i) to propose additional theoretical insight into the time irreversibility characterization method of Costa *et al* (2005), in order to better appreciate its capabilities, expected behaviors and limitations; (ii) to undertake the first application to study the time reversibility/irreversibility properties of LDF and LDF_R_{ECG} data; (iii) to analyze the results obtained with LDF and LDF_R_{ECG} signals and confront them with those found from signals reflecting the central CVS (HRV data) recorded simultaneously to LDF signals.

2. Theoretical analysis of a time irreversibility characterization method

2.1. Characterization of time irreversibility

The method proposed by Costa *et al* (2005) for the characterization of time irreversibility is presented is this section. Costa *et al* used a discrete approach with a time series $X = \{x_i\}$, $1 \leqslant i \leqslant N$, where N is the number of samples in the data. We will herein extend to the continuous case and, to this purpose, our random signal will be denoted as $X(t)$.

Costa *et al* (2005) first proposed the computation of a time series of the one-step difference $Y = \{y_i\}$ as $y_i = x_{i+1} - x_i$, $1 \leqslant i \leqslant N-1$. Then, this time series $\{y_i\}$ of the one-step difference is aggregated to yield the coarse-grained time series $\{y_\tau(i)\}$ defined as (Costa *et al* 2005)

$$y_\tau(i) = \frac{1}{\tau} \sum_{j=0}^{\tau-1} y_{i+j}. \tag{1}$$

These two steps can be directly gathered by determining the time series $Y_\tau(t)$ of the increments as (in the continuous domain)

$$Y_\tau(t) = \frac{X(t+\tau) - X(t)}{\tau}. \tag{2}$$

Costa *et al* (2005) then introduced a probability density function $\rho(y_\tau)$ for the increment Y_τ, and they defined a measure of temporal irreversibility, based on a separate treatment of the positive and negative increments, through

$$a(\tau) = \frac{\int_0^\infty [\rho(y_\tau) \ln(\rho(y_\tau)) - \rho(-y_\tau) \ln(\rho(-y_\tau))]^2 \, dy_\tau}{\int_{-\infty}^\infty \rho(y_\tau) \ln(\rho(y_\tau)) \, dy_\tau}. \tag{3}$$

According to Costa *et al*, a time series is reversible if and only if $a(\tau) = 0$, as deduced from a symmetry in the positive and negative increments.

In order to distinguish the forward and backward directions in time, Costa *et al* (2005) further considered

$$A(\tau) = \frac{\int_0^\infty [\rho(y_\tau) \ln(\rho(y_\tau)) - \rho(-y_\tau) \ln(\rho(-y_\tau))] \, dy_\tau}{\int_{-\infty}^\infty \rho(y_\tau) \ln(\rho(y_\tau)) \, dy_\tau} \tag{4}$$

instead of (3), and they mentioned that if $A(\tau) > 0$, then for this τ the time series is irreversible, as revealed by a lack of a symmetry in the positive and negative increments.

For application of their irreversibility indices to empirically observed signals, Costa *et al* (2005) then turned to discrete-valued variables and an estimator of $A(\tau)$ as

$$\hat{A}(\tau) = \frac{\sum_{y_\tau > 0} \Pr(y_\tau) \ln[\Pr(y_\tau)]}{\sum_{y_\tau} \Pr(y_\tau) \ln[\Pr(y_\tau)]} - \frac{\sum_{y_\tau < 0} \Pr(y_\tau) \ln[\Pr(y_\tau)]}{\sum_{y_\tau} \Pr(y_\tau) \ln[\Pr(y_\tau)]}, \tag{5}$$

where $\Pr(y_\tau)$ is the probability of the value y_τ.

Costa *et al* (2005) then defined an asymmetry index A_I as the sum

$$A_I = \sum_{\tau=1}^{L} \hat{A}(\tau). \tag{6}$$

This A_I index is convenient since it offers a single scalar value to summarize the irreversibility properties. It may however bear some dependence with the time horizon L considered for the analysis. This feature also interacts with the form of (2) containing a division by τ of the increments, which tends to wipe out long-term increments associated with large τ, and could thus mitigate the dependence with L of (6). However, equation (4) or (5) through their denominator induces some sort of normalization by the range of the increments, which would

tend to restore a dependence with L of (6). We will therefore concentrate our forthcoming analysis on the index $\hat{A}(\tau)$ as a function of τ and prior to its aggregation according to (6).

In Costa *et al* (2005), the indices $\hat{A}(\tau)$ and A_I, after their definition as above, were directly applied to the analysis of measured physiologic time series, to draw conclusion on their irreversibility properties. As a complement, we propose herein an analysis of the properties of this approach based on different models of reference for random signals, for which we analytically investigate the theoretical behavior and capabilities.

2.2. Characterization method on signal models

Let $X(t)$ be a random signal and $p_X(x, t)$ its probability density function. We consider the increment signal $Y_\tau(t) = X(t + \tau) - X(t)$, where, compared to (2), we omit the division by τ which does not interact with the time irreversibility of $X(t)$. The probability density function of the increment $Y_\tau(t)$ is denoted as $p_{Y_\tau}(y, t)$.

It is interesting to relate and express the irreversibility characterization of Costa *et al* (2005) based on (4) or (5), in terms of the standard notion of differential entropy of a random variable (Cover and Thomas 1991). In this way, we introduce for the increment $Y_\tau(t)$ the entropy

$$H[Y_\tau(t)] = -\int_{-\infty}^{+\infty} p_{Y_\tau}(y, t) \ln(p_{Y_\tau}(y, t)) \mathrm{d}y. \tag{7}$$

For the positive increments $Y_\tau^+(t)$, we have a probability density function $p_{Y_\tau}^+(y, t)$ equal to

$$p_{Y_\tau}^+(y, t) = \frac{1}{P^+(t)} p_{Y_\tau}(y, t), \qquad \text{for } y \geqslant 0 \text{ only}, \tag{8}$$

while $p_{Y_\tau}^+(y, t) = 0$ for $y < 0$. In (8), we have the probability $P^+(t) = \int_0^{+\infty} p_{Y_\tau}(y, t) \, \mathrm{d}y$ which is necessary for a proper normalization of the density $p_{Y_\tau}^+(y, t)$. The corresponding entropy $H[Y_\tau^+(t)]$ for the positive increments $Y_\tau^+(t)$ follows as

$$H[Y_\tau^+(t)] = -\int_0^{+\infty} p_{Y_\tau}^+(y, t) \ln\left(p_{Y_\tau}^+(y, t)\right) \mathrm{d}y. \tag{9}$$

For the negative increments $Y_\tau^-(t)$, we have in a similar way the probability density

$$p_{Y_\tau}^-(y, t) = \frac{1}{P^-(t)} p_{Y_\tau}(y, t), \qquad \text{for } y \leqslant 0 \text{ only}, \tag{10}$$

with $P^-(t) = \int_{-\infty}^0 p_{Y_\tau}(y, t) \, \mathrm{d}y$, and the entropy

$$H[Y_\tau^-(t)] = -\int_{-\infty}^0 p_{Y_\tau}^-(y, t) \ln\left(p_{Y_\tau}^-(y, t)\right) \mathrm{d}y. \tag{11}$$

A composition relation exists between the three above entropies, which reads

$$H[Y_\tau(t)] = P^-(t)H[Y_\tau^-(t)] + P^+(t)H[Y_\tau^+(t)] + H_{\text{bin}}[P^-(t), P^+(t)], \tag{12}$$

where $H_{\text{bin}}[P^-(t), P^+(t)] = -P^-(t) \ln[P^-(t)] - P^+(t) \ln[P^+(t)]$.

By comparison, equation (4) or (5) for the positive and negative increments rather uses partial entropies which are expressed with non-normalized probability densities. In this respect, equation (4) is

$$A(\tau) = \frac{H_{\text{par}}[Y_\tau^-(t)] - H_{\text{par}}[Y_\tau^+(t)])}{H[Y_\tau(t)]}, \tag{13}$$

with the partial entropies

$$H_{\text{par}}[Y_\tau^+(t)] = -\int_0^{+\infty} p_{Y_\tau}(y, t) \ln(p_{Y_\tau}(y, t)) \mathrm{d}y, \tag{14}$$

and

$$H_{\mathrm{par}}[Y_\tau^-(t)] = -\int_{-\infty}^0 p_{Y_\tau}(y,t)\ln(p_{Y_\tau}(y,t))\,\mathrm{d}y, \tag{15}$$

and $H_{\mathrm{par}}[Y_\tau^-(t)] + H_{\mathrm{par}}[Y_\tau^+(t)] = H[Y_\tau(t)]$. Yet these partial entropies of (14) and (15) relate to the regular entropies of (9) and (11) through

$$H_{\mathrm{par}}[Y_\tau^+(t)] = P^+(t)H[Y_\tau^+(t)] - P^+(t)\ln[P^+(t)], \tag{16}$$

and

$$H_{\mathrm{par}}[Y_\tau^-(t)] = P^-(t)H[Y_\tau^-(t)] - P^-(t)\ln[P^-(t)]. \tag{17}$$

Alternatively, equation (4) suggests another symmetry index for irreversibility, but based on regular entropies, as

$$A'(\tau) = \frac{H[Y_\tau^-(t)] - H[Y_\tau^+(t)]}{H[Y_\tau(t)]}. \tag{18}$$

This index $A'(\tau)$ has the benefit of a point of view on irreversibility based on a standard notion of entropy with known properties and an informational interpretation.

In the following, we use the common and standard notion of entropy, so as to express the index $A(\tau)$ or $A'(\tau)$ for different signal models, and through their analytical expressions test their properties for the characterization of time irreversibility.

2.2.1. Case of white fluctuations. We consider $X(t)$ a white fluctuation with probability density $p_X(x,t)$. Then the increment $Y_\tau(t) = X(t+\tau) - X(t)$ has a probability density $p_{Y_\tau}(y,t)$ given by the convolution $p_{Y_\tau}(y,t) = p_X(x,t+\tau) * p_X(-x,t)$, or

$$p_{Y_\tau}(y,t) = \int_{-\infty}^{+\infty} p_X(x,t+\tau)p_X(x-y,t)\,\mathrm{d}x. \tag{19}$$

As a result, for the argument $-y$ and through a change of variable in (19), one has

$$p_{Y_\tau}(-y,t) = \int_{-\infty}^{+\infty} p_X(x'-y,t+\tau)p_X(x',t)\,\mathrm{d}x'. \tag{20}$$

We conclude that when $X(t)$ is a *stationary* white fluctuation, then $p_X(x,t+\tau) = p_X(x,t) = p_X(x)$, and therefore $p_{Y_\tau}(y,t) = p_{Y_\tau}(-y,t)$ follows as an even probability density independent of t and τ. It then follows that $P^+ = P^- = 1/2$ and $H[Y_\tau^+] = H[Y_\tau^-] = H[Y_\tau] - 1$ bit. In this case, from (13) and (18), we have the indices $A(\tau) = 0$ and $A'(\tau) = 0$, at any scale τ. Therefore, a stationary white fluctuation is always characterized as time reversible by the indices $A(\tau)$ and $A'(\tau)$, at any scale τ. Possible asymmetry in the positive or negative excursions of the fluctuation $X(t)$, associated with an asymmetric probability density $p_X(x)$, will be wiped out in the time series of the increments Y_τ and has no influence in the entropy measures of (13) and (18). This is a desirable behavior of the irreversibility indices $A(\tau)$ and $A'(\tau)$ to vanish in this case, because a stationary white fluctuation conforms indeed to the notion of a time reversible signal.

As in Costa *et al* (2005), a non-zero value for the index $A(\tau)$ or $A'(\tau)$ here identifies an irreversible fluctuation. Also, as in Costa *et al* (2005), when the index $A(\tau) = 0$ or $A'(\tau) = 0$, then in general the fluctuation may or may not be reversible. However, an irreversible fluctuation with zero indices could be expected to have a specifically sophisticated constitution. Zero indices for such an irreversible fluctuation would express that there is no asymmetry in the positive and negative increments. Any time irreversibility should therefore come from higher order statistical properties not visible from the probability distributions of the increments. For the model signal formed by the stationary white fluctuation here,

$A(\tau) = 0$ and $A'(\tau) = 0$ that we found are taken as a mark of reversibility of this signal. This is because the stationary white fluctuation has no correlation, no higher order statistical structure and therefore the zero value of the indices is sufficient to establish reversibility.

Next, it is useful to explore the expected behavior of the irreversibility indices when we move to other, more structured, signal models. We shall first examine the impact of correlation on the temporal fluctuation $X(t)$, and for the sake of an analytically tractable situation, we examine the behavior of the irreversibility indices on a Gaussian stationary colored fluctuation.

2.2.2. Case of Gaussian stationary colored fluctuations. We consider $X(t)$ a stationary Gaussian fluctuation with mean m_X, standard deviation σ_X and a correlation structure specified by the normalized cross-covariance $\rho(\tau)$. In such a case, the increment $Y_\tau(t) = X(t+\tau) - X(t)$ is zero-mean Gaussian with standard deviation $\sigma_{Y_\tau} = \sqrt{2}\sigma_X\sqrt{1 - \rho(\tau)}$ (Papoulis 1991). It then follows that $P^+ = P^- = 1/2$ and $H[Y_\tau^+] = H[Y_\tau^-] = H[Y_\tau] - 1$ bit, with the entropy of the Gaussian increment

$$H[Y_\tau] = \ln(\sqrt{2\pi e}\,\sigma_{Y_\tau}) = H[X(t)] + \tfrac{1}{2}\ln[1 - \rho(\tau)] + \tfrac{1}{2}\ln(2). \tag{21}$$

In this case, from (13) and (18), we have the indices $A(\tau) = 0$ and $A'(\tau) = 0$, for any correlation structure $\rho(\tau)$. Therefore, a Gaussian stationary colored fluctuation is always characterized as time reversible by the indices $A(\tau)$ and $A'(\tau)$. This is again a desirable behavior of the irreversibility indices $A(\tau)$ and $A'(\tau)$ to vanish in this case, because a Gaussian stationary colored fluctuation conforms indeed to the notion of a time reversible signal.

To investigate further generic conditions where some irreversibility would be present in a reference signal model and captured by the index $A(\tau)$ or $A'(\tau)$, we now turn to the case of nonstationary fluctuations.

2.2.3. Case of stationary white fluctuation deterministically modulated. As a generic and tractable model for a nonstationary random signal $X(t)$, we will consider a stationary white fluctuation modulated in time by a deterministic signal $s(t)$.

Let $s(t)$ be a deterministic signal and $B(t)$ a stationary white noise with probability density function $f_B(u)$.

- *Case of stationary white fluctuation with multiplicative modulation.* We consider $X(t) = s(t)B(t)$ coming with the nonstationary probability density $p_X(x, t) = f_B[x/s(t)]/s(t)$. The increment $Y_\tau(t) = X(t + \tau) - X(t)$ follows with a probability density $p_{Y_\tau}(y, t)$ given by the convolution (Papoulis 1991) $p_{Y_\tau}(y, t) = f_B[x/s(t+\tau)]/s(t+\tau) * f_B[-x/s(t)]/s(t)$, or

$$p_{Y_\tau}(y, t) = \frac{1}{s(t)s(t + \tau)} \int_{-\infty}^{+\infty} f_B\left(\frac{-x}{s(t)}\right) f_B\left(\frac{y - x}{s(t + \tau)}\right) dx. \tag{22}$$

From (22) and a change of variable, we also have

$$p_{Y_\tau}(-y, t) = \frac{1}{s(t)s(t + \tau)} \int_{-\infty}^{+\infty} f_B\left(\frac{x'}{s(t)}\right) f_B\left(\frac{x' - y}{s(t + \tau)}\right) dx', \tag{23}$$

showing that in general $p_{Y_\tau}(-y, t) \neq p_{Y_\tau}(y, t)$ and thus the probability density $p_{Y_\tau}(y, t)$ is not an even function. This general case when $p_{Y_\tau}(y, t)$ is not an even density will usually entail (except for some very specific densities) $P^+(t) \neq P^-(t)$, also $H_{par}[Y_\tau^+(t)] \neq H_{par}[Y_\tau^-(t)]$, and $H[Y_\tau^+(t)] \neq H[Y_\tau^-(t)]$. As a result, the irreversibility indices $A(\tau)$ and $A'(\tau)$ from (13) and (18) will generally be non-zero, although their specific values will depend on the time t at which they are evaluated. In this way, the nonstationary signal

$X(t)$ realized by a white fluctuation $B(t)$ multiplicatively modulated by a deterministic signal $s(t)$ will generally be characterized as an irreversible signal by the index $A(\tau)$ or $A'(\tau)$.

One can also think of some stationarization process that could result from an empirical evaluation of the index $A(\tau)$ or $A'(\tau)$ from the increments $Y_\tau(t)$ observed on a single temporal realization of $X(t)$. This would in general induce some stationarization process on the underlying nonstationary density $p_{Y_\tau}(y, t)$, which would be empirically evaluated as a stationary density $p_{Y_\tau}(y) = \langle p_{Y_\tau}(y, t) \rangle$. For instance, if the deterministic modulation $s(t)$ has a period T, then the stationarization of the density will occur through a time average $\langle \cdot \rangle = T^{-1} \int_0^T \cdot \, \mathrm{d}t$. Since each nonstationary density $p_{Y_\tau}(y, t)$ is in general a non-even function for any t, stationarization or time averaging over t of such non-even densities will still result in a non-even stationary density $p_{Y_\tau}(y)$ (except maybe for some very specific modulation $s(t)$). And from a non-even stationary density $p_{Y_\tau}(y)$, the resulting irreversibility index $A(\tau)$ or $A'(\tau)$ will generally be non-zero, still characterizing the signal $X(t)$ as irreversible.

These non-vanishing behaviors of the irreversibility index $A(\tau)$ or $A'(\tau)$ however break down in the special case where the white noise $B(t)$ has a symmetric even probability density $f_B(u)$. In this case, from (23) it results that $p_{Y_\tau}(-y, t) = p_{Y_\tau}(y, t)$ and thus the probability density $p_{Y_\tau}(y, t)$ also is an even function. This entails $P^+(t) = P^-(t) = 1/2$, also $H_{\mathrm{par}}[Y_\tau^+(t)] = H_{\mathrm{par}}[Y_\tau^-(t)]$, and $H[Y_\tau^+(t)] = H[Y_\tau^-(t)]$. As a result, the irreversibility indices $A(\tau)$ and $A'(\tau)$ from (13) and (18) vanish at any time t and increment τ. In this way, the nonstationary signal $X(t)$ realized by a symmetric white fluctuation multiplicatively modulated by a deterministic signal $s(t)$ will generally be characterized as a reversible signal by the index $A(\tau)$ or $A'(\tau)$.

- *Case of stationary white fluctuation with additive modulation.* We consider $X(t) = s(t) + B(t)$ coming with the nonstationary probability density $p_X(x, t) = f_B[x - s(t)]$. The increment $Y_\tau(t) = X(t + \tau) - X(t)$ follows with a probability density $p_{Y_\tau}(y, t)$ given by the convolution (Papoulis 1991) $p_{Y_\tau}(y, t) = f_B[x - s(t + \tau)] * f_B[s(t) - x]$. Alternatively, since $Y_\tau(t) = B(t + \tau) - B(t) + s(t + \tau) - s(t)$, the density $p_{Y_\tau}(y, t)$ of the increment $Y_\tau(t)$ will be given by the density of $B(t + \tau) - B(t)$; let us call it $f_{B-B}(u)$, affected by a shift of $s(t + \tau) - s(t)$ in the mean, i.e. $p_{Y_\tau}(y, t) = f_{B-B}[y - s(t + \tau) + s(t)]$. Since $B(t)$ is a stationary white noise, by the same reasons expressed by (19) and (20), the density $f_{B-B}(u)$ is always an even function. However, due to the shift in the mean, the density $p_{Y_\tau}(y, t) = f_{B-B}[y - s(t + \tau) + s(t)]$ of the increment will not generally be an even function. This will usually entail the same consequences as for the multiplicative modulation (except for some very specific densities): $P^+(t) \neq P^-(t)$, also $H_{\mathrm{par}}[Y_\tau^+(t)] \neq H_{\mathrm{par}}[Y_\tau^-(t)]$, and $H[Y_\tau^+(t)] \neq H[Y_\tau^-(t)]$. As a result, the irreversibility indices $A(\tau)$ and $A'(\tau)$ from (13) and (18) will generally be non-zero, although their specific values will depend on the time t at which they are evaluated. In this way, the nonstationary signal $X(t)$ realized by a white fluctuation $B(t)$ additively modulated by a deterministic signal $s(t)$ will generally be characterized as an irreversible signal by the index $A(\tau)$ or $A'(\tau)$.

For confrontation with an empirical evaluation from a single temporal realization of $X(t)$, stationarization of the non-even time-dependent density $p_{Y_\tau}(y, t)$ will usually produce a non-even stationary density $p_{Y_\tau}(y)$ and ultimately, non-zero irreversibility index $A(\tau)$ or $A'(\tau)$, still characterizing the signal $X(t)$ as irreversible.

From these theoretical elements, we now process LDF, LDF_R$_{\mathrm{ECG}}$ and HRV data with the time irreversibility characterization method.
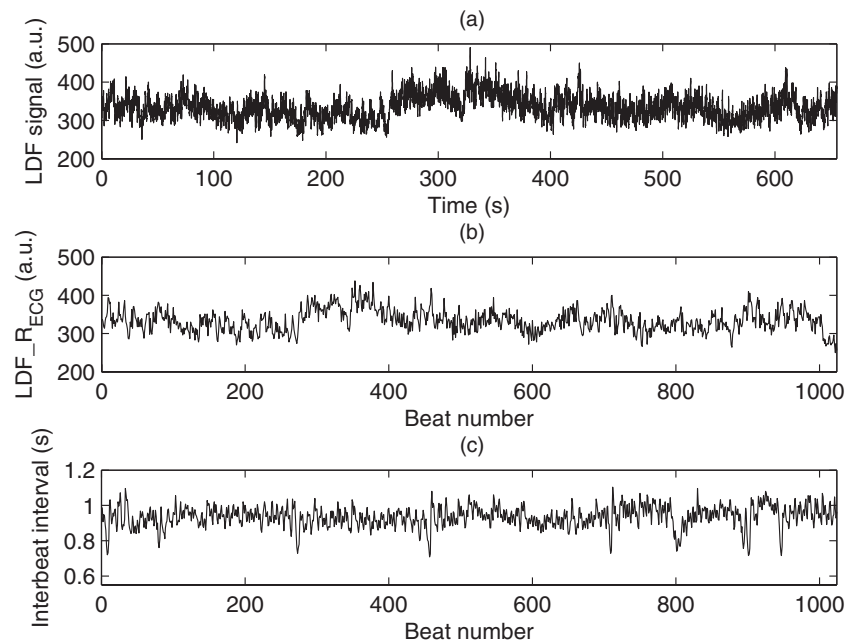
Figure 1. (a) LDF signal recorded on the forearm of a healthy subject. The sampling period is 40 ms. (b) LDF signal reduced to samples acquired during the R peaks of the ECG (LDF_R_{ECG} signal) on a healthy subject. (c) HRV signal of a healthy subject.

3. Materials and methods

3.1. Measurement procedure

Thirteen subjects (mean age 29.2 ± 11.5 years; four women) without known disease participated in the study. All volunteers provided written, informed consent prior to participation and the study was carried out in accordance with the Declaration of Helsinki. Subjects were placed supine in a quiet room with the ambient temperature set at 23 ± 1 °C. For temperature and cardiovascular adaptations, the subjects were left at rest for 15 min before each measurement. A laser Doppler probe (PF408, Perimed; fiber separation equal to 0.25 mm) connected to a laser Doppler flowmeter (Periflux PF4001, Perimed) was used to record LDF signals. The LDF probe was positioned on the forearm ventral face of the subjects. The measurement depth was therefore around 1 mm (O'Doherty *et al* 2009). Skin blood flow was assessed in arbitrary units (au) and recorded on a computer via an analog-to-digital converter (Biopac System) with a sampling frequency of 250 Hz. A sub-sampling to 25 Hz was then performed. For the ECG acquisition, a Lifescope (Nihon Kohden Corporation) was used, and the signals were recorded with a sampling frequency of 1000 Hz and then sub-sampled to 250 Hz. In our work, LDF and ECG signals were recorded simultaneously for 20 min.

After acquisition, ECG signals were processed to obtain the HRV data: a computer program was developed by our group (written in Matlab, The MathWorks, Inc) to automatically detect the R peaks of the ECG time series; the results given by the automatic detection were then visually checked and corrected if needed, and the R–R intervals were computed. Moreover, LDF signals reduced to samples acquired during the R peaks of the ECG (LDF_R_{ECG} signals) were also generated. Examples of LDF, LDF_R_{ECG} and HRV data are shown in figure 1.
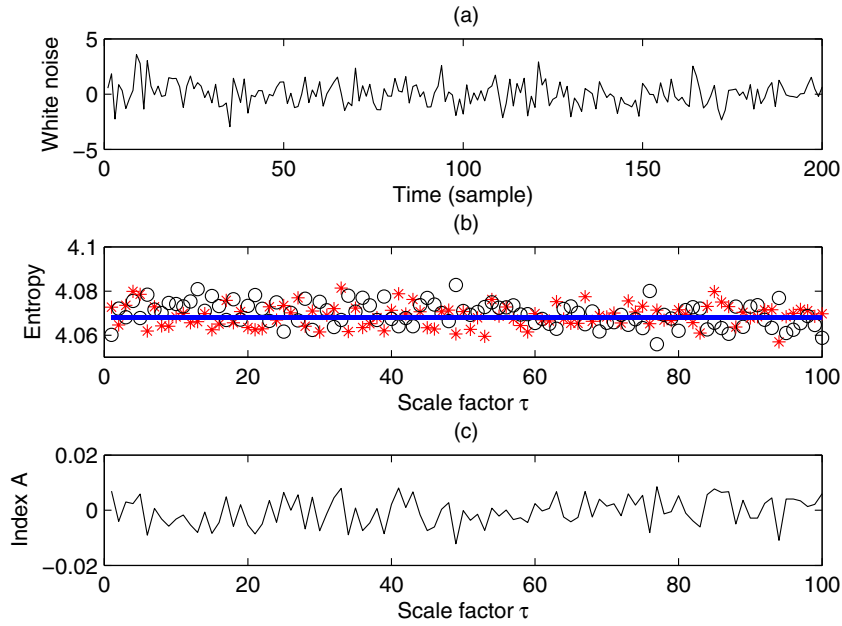
Figure 2. (a) Gaussian white noise with mean 0 and standard deviation equal to 1. Only 200 samples over 60 000 are shown. The sampling period is chosen equal to 1 sample. The corresponding time series can be considered as time reversible. (b) Entropies for the positive ($*$) and negative ($\circ$) increments ($H[Y_\tau^+]$ and $H[Y_\tau^-]$, respectively) computed from the signal in (a), for each scale factor τ. The solid line corresponds to the theoretical value for entropies. The bin size is 0.05. (c) Evolution of asymmetry index $\hat{A}(\tau)$ with scale factor τ for the signal presented in (a). (b), (c) The sampling period of the signal being 1 sample, for scale factors τ going from 1 to 100 we have time scales ranging from 1 to 100 samples.

3.2. Signal processing method

In what follows, our physiological signals are denoted as $X = \{x(i)\}$, $1 \leqslant i \leqslant N$, where N is the number of samples in the data. Based on theoretical backgrounds mentioned above, we first determine the increments $Y_\tau = \{y_\tau(i)\}$, $1 \leqslant i \leqslant N - 1$, of the signal X by computing $y_\tau(i) = x(i + \tau) - x(i)$. Then, the entropy $H[Y_\tau]$ for the increments Y_τ, the entropy $H[Y_\tau^+]$ for the positive increments Y_τ^+ and the entropy $H[Y_\tau^-]$ for the negative increments Y_τ^- are computed. Entropies are computed as

$$H[Y_\tau] = -\sum_{y_\tau} \Pr(y_\tau) \ln[Pr(y_\tau)], \tag{24}$$

where $\Pr(y_\tau)$ corresponds to the probability of $y_\tau(i)$. To determine the latter probability, the histogram of each time series Y_τ was computed with a bin size denoted as *bin*. The discrete version of the entropy $H[Y_\tau] = H^{\text{dis}}[Y_\tau]$ of (24) based on the discrete probabilities $\Pr(y_\tau)$ and used for experimental evaluation is related to the continuous entropy $H[Y_\tau(t)] = H^{\text{cont}}[Y_\tau(t)]$ of (7) through the relation $H^{\text{cont}}[Y_\tau(t)] \approx H^{\text{dis}}[Y_\tau] + \ln(\text{bin})$ (Cover and Thomas 1991). The continuous entropy $H[Y_\tau(t)] = H^{\text{cont}}[Y_\tau(t)]$ of (7) is intrinsic to the fluctuation $Y_\tau(t)$ and determined by its probability density $p_Y(y)$. By contrast, the discrete entropy $H[Y_\tau] = H^{\text{dis}}[Y_\tau]$ of (24) is dependent on the precision bin $= \Delta y$ used to quantize the fluctuation $Y_\tau(t)$ and measure probabilities $\Pr(y_\tau) \approx p_Y(y_\tau)\Delta y$. Accordingly, when using the discrete entropy
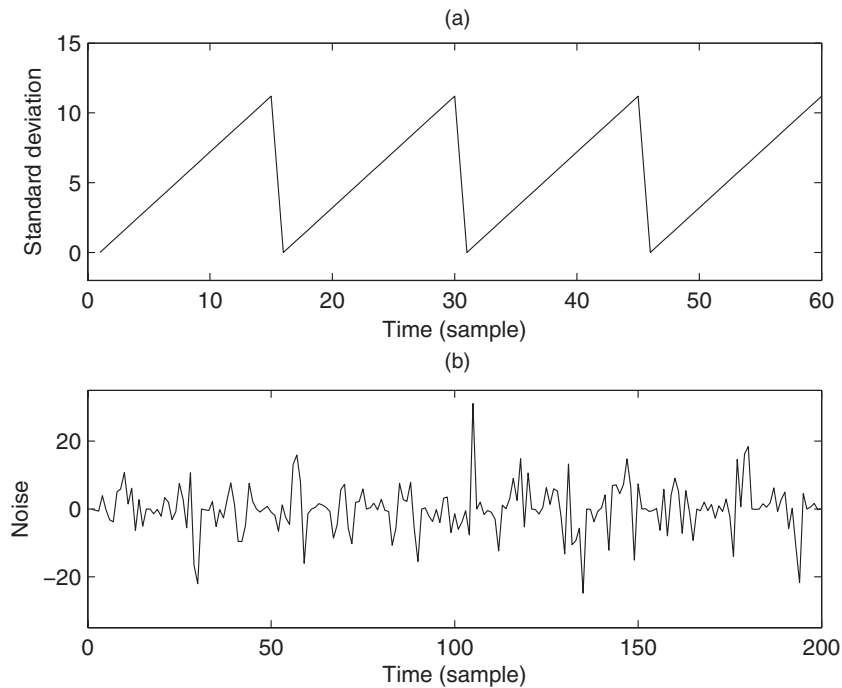
Figure 3. (a) Evolution of the standard deviation for the white noise processed. The triangle pattern has 15 samples and is periodically repeated all along the signal. (b) Gaussian white noise with mean 0 and standard deviation presented in (a). Only 200 samples over 60 000 are shown. The sampling period is chosen equal to 1 sample. The corresponding time series can be considered as time irreversible.

$H[Y_\tau]$ of (24), we have the possibility of an irreversibility index independent of the (small) experimental precision bin $= \Delta y$ as

$$\widehat{A}(\tau) = \frac{H[Y_\tau^+] - H[Y_\tau^-]}{H[Y_\tau] + \ln(\text{bin})}. \tag{25}$$

The precision bin $= \Delta y$ is the same for the experimental evaluation of $H[Y_\tau^+]$ and $H[Y_\tau^-]$, and thus the common factor $\ln(\text{bin}) = \ln(\Delta y)$ disappears at the numerator of (25) in the difference of two entropies, while it remains in the entropy of the denominator. In this way, we have with (25) an irreversibility index independent of the (small) experimental precision bin $= \Delta y$, while the original form of the index introduced in Costa *et al* (2005) with no factor $\ln(\text{bin})$ at the denominator will depend on the experimental precision bin $= \Delta y$ with which the fluctuation is quantized. Now, in the present framework of interpretation, for a given scale factor τ, the closer $\widehat{A}(\tau)$ is to zero, the more reversible is the original time series at this scale factor τ.

In what follows, to validate our processing approach, we first apply it to two kinds of numerically generated synthetic signals—having known statistical properties—before application to physiological signals. The first synthetic signal is a Gaussian white noise with mean 0 and standard deviation 1 (see figure 2(a)). Qualitatively, this signal can be considered as a reversible time series. The second synthetic signal is a Gaussian white noise with mean 0 and a standard deviation following a periodic triangle law (see figure 3). Qualitatively, this
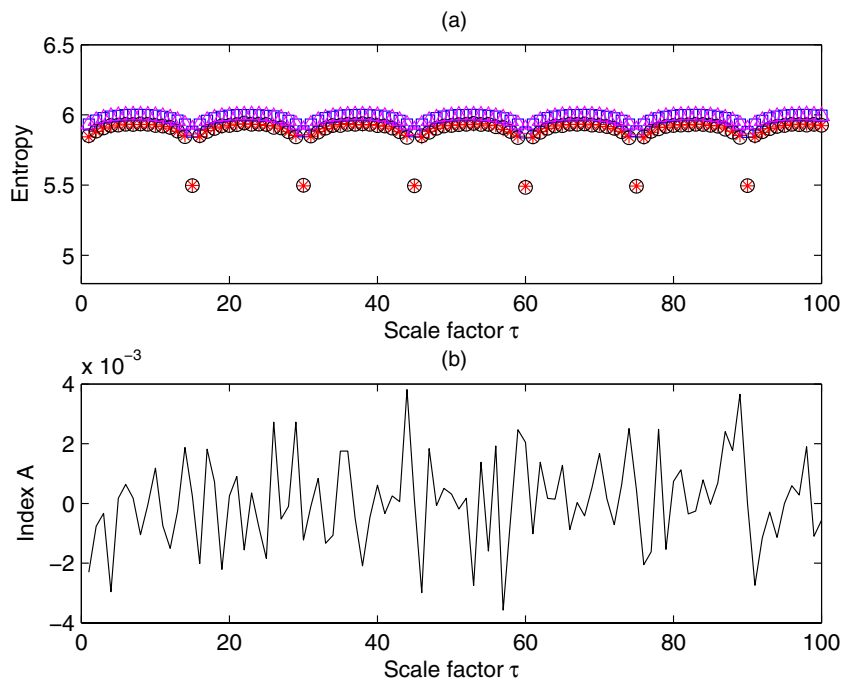
Figure 4. (a) ○ and ∗: numerically estimated (from histograms) entropies $H[Y_\tau^+]$ of positive increments and $H[Y_\tau^-]$ of negative increments for the Gaussian white noise presented in figure 3(b). □ and △: theoretical values for $H[Y_\tau^+]$ and $H[Y_\tau^-]$. The bin size is 0.05. (b) Evolution of asymmetry index $\hat{A}(\tau)$ with scale factor τ for the signal presented in figure 3(b). (a), (b) The sampling period of the signal being 1 sample, for scale factors τ going from 1 to 100 we have time scales ranging from 1 to 100 samples.

second synthetic signal can be seen as an irreversible time series. These two synthetic time series possess 60 000 samples.

4. Results and discussion

In what follows, the bin value used in the histogram for the entropy computation has been chosen to be higher than the lowest value between two samples but low enough to obtain histograms with smooth edges. This led to a bin value of 0.05 for both the synthetic signals and the experimental LDF, LDF_R$_{\text{ECG}}$ and HRV data. The results obtained for the two numerically generated synthetic signals are presented in figures 2 and 4, respectively. For the Gaussian white noise with mean 0 and standard deviation equal to 1, we note that entropies for positive and negative increments, $H[Y_\tau^+]$ and $H[Y_\tau^-]$, respectively, are close to each other for a given scale factor τ (see figure 2). Their value is close to 4.070. These results are the expected ones as for a white noise with mean 0 and standard deviation 1 having a Gaussian probability density function, the entropies for positive and negative increments are

$$H[Y_\tau^+] = H[Y_\tau^-] = \ln\left(\sigma_{y_\tau}\sqrt{\frac{e\pi}{2}}\right) - \ln(\text{bin}) = 4.068 \qquad \text{(in nats)}, \qquad (26)$$
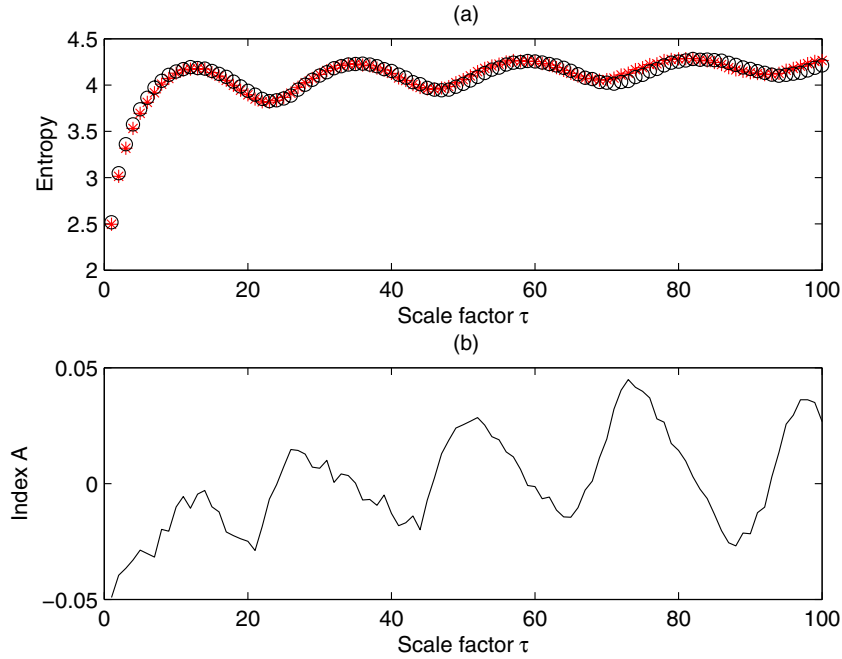
Figure 5. (a) Entropy for the positive (∗) and negative (○) increments ($H[Y_\tau^+]$ and $H[Y_\tau^-]$, respectively) computed from the LDF signal of figure 1(a), for each scale factor τ. The bin size is 0.05. (b) Evolution of asymmetry index $\hat{A}(\tau)$ with scale factor τ for the signal presented in figure 1(a). (a), (b) The sampling period of the LDF signal being 40 ms, for scale factors τ going from 1 to 100 we have time scales ranging from 0.04 to 4 s.

where σ_{y_τ} is the standard deviation of the increment time series Y_τ. We also note that the asymmetry index $\hat{A}(\tau)$ wanders around 0; $\hat{A}(\tau)$ values go between -0.012 and 0.008 when scale factors τ go from 1 to 100.

For the Gaussian white noise with mean 0 and standard deviation following a triangle law (see figure 3), we observe that positive and negative increments, Y_τ^+ and Y_τ^-, respectively, have entropies that are close to each other for a given scale factor τ (see figure 4). These entropies, $H[Y_\tau^+]$ and $H[Y_\tau^-]$, have the same pattern which presents a periodic behavior. The period for these entropies is equal to the one of the signal standard deviations (triangle length; see figure 3(a)). These results are also the ones expected as for this second synthetic signal being Gaussian and having a standard deviation following a periodic law, the probability density functions for the increment time series Y_τ are

$$\text{pdf}(u, \tau) = \frac{1}{T} \int_0^T \frac{1}{\sigma_{y_\tau}(t, \tau) \times \sqrt{2 \times \pi}} \times \exp\left(\frac{-(u - \overline{m})^2}{2 \times \sigma_{y_\tau}^2(t, \tau)}\right) \mathrm{d}t, \qquad (27)$$

where σ_{y_τ} is the standard deviation of the increment time series Y_τ and $\overline{m}$ is the mean value of the increment signal. From these probability density functions, the theoretical entropies for positive and negative increments, $H[Y_\tau^+]$ and $H[Y_\tau^-]$, respectively, are shown in figure 4(a). They correspond to the ones computed through histograms. Moreover, the asymmetry index $\hat{A}(\tau)$ wanders around 0; $\hat{A}(\tau)$ values go between -0.003 and 0.004 when scale factors τ go from 1 to 100 (see figure 4(b)). For the first and second synthetic signals, respectively reversible and irreversible signal, the computed entropies $H[Y_\tau^+]$ and $H[Y_\tau^-]$ for positive and
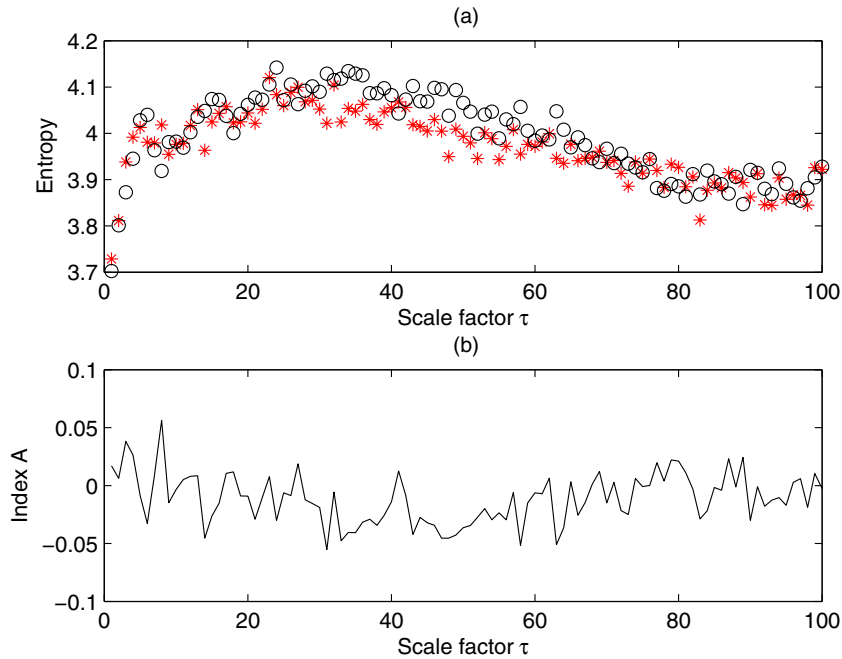
Figure 6. (a) Entropy for the positive (∗) and negative (○) increments ($H[Y_\tau^+]$ and $H[Y_\tau^-]$, respectively) computed from the LDF_R_{ECG} signal of figure 1(b), for each scale factor τ. (b) Evolution of asymmetry index $\hat{A}(\tau)$ with scale factor τ for the signal presented in figure 1(b).

negative increments correspond to the ones found theoretically. Our approach is thus thereafter applied to LDF, LDF_R_{ECG} and HRV experimental data.

Due to the high sensitivity of the LDF technique to movements (movements of the subjects, optical fiber movements, movements of the probe head relative to the tissue, etc), the subject has to be completely still during the acquisition. Therefore, the process of long LDF recordings is not possible if we want data that do not contain any movement artifact. For each LDF signal, 16 384 samples are herein processed (∼11 min of data). For LDF_R_{ECG} and HRV data, 1024 samples are taken into account (this corresponds to a mean of 14.5 min for our 13 subjects). Results obtained with LDF and LDF_R_{ECG} signals are presented in figures 5 and 6, respectively. We observe that the entropy $H[Y_\tau^+]$ for the positive increments Y_τ^+ and the entropy $H[Y_\tau^-]$ for the negative increments Y_τ^- of LDF signals present oscillations. By computing the period of these oscillations and comparing the results with the period of the cardiac activity (mean of HRV data), for each subject, we note that they are equal. The amplitude of these oscillations varies from one subject to another and decreases when the scale factor τ increases. Moreover, we observe that, for some of our subjects, oscillations are also visible on the asymmetry index $\hat{A}(\tau)$ curve (see examples in figure 5(b)). The amplitude of these oscillations also differs between subjects. Furthermore, when LDF signals are reduced to samples acquired during the R peaks of the ECG data (LDF_R_{ECG} signals), the oscillations with period of the cardiac activity are not present any more on the entropy $H[Y_\tau^+]$ of the positive increments Y_τ^+ nor on the entropy $H[Y_\tau^-]$ of the negative increments Y_τ^- (see an example in figure 6(a)). This is true for all our subjects. By definition, LDF_R_{ECG} signals do not contain the dominant frequency of the heart beat (see for example Lotric *et al* 2000). That is why the
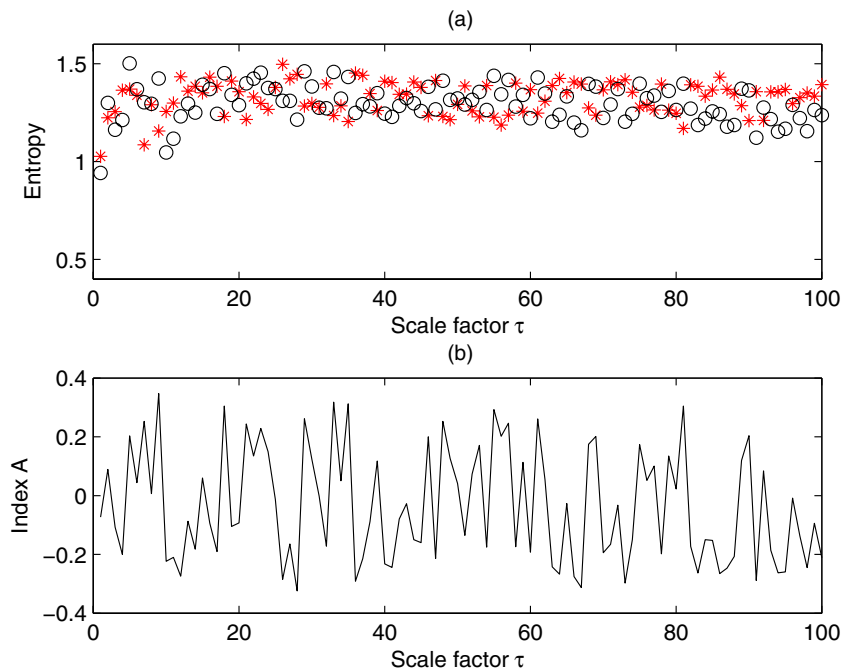
Figure 7. (a) Entropy for the positive ($*$) and negative ($\circ$) increments ($H[Y_\tau^+]$ and $H[Y_\tau^-]$, respectively) computed from the HRV signal of figure 1(c), for each scale factor τ. The bin size is 0.05. (b) Evolution of asymmetry index $\hat{A}(\tau)$ with scale factor τ for the signal presented in figure 1(c).

oscillations with period of the cardiac activity are not present any more on the entropy $H[Y_\tau^+]$ nor on the entropy $H[Y_\tau^-]$ of these data. The entropy $H[Y_\tau^+]$ and the entropy $H[Y_\tau^-]$ present an increasing trend and then they tend to decrease (see an example in figure 6(a)). Moreover, for LDF_R$_{ECG}$ signals, the asymmetry index $\hat{A}(\tau)$ wanders around 0, in a way similar to the one observed for the Gaussian white noises (see figure 6(b)).

For HRV data, the entropy $H[Y_\tau^+]$ for the positive increments Y_τ^+ and the entropy $H[Y_\tau^-]$ for the negative increments Y_τ^- are almost constant for scale factors τ lower than 15, but seem to present an increasing trend due to the low values of the entropies $H[Y_\tau^+]$ and $H[Y_\tau^-]$ for $\tau = 1$; for higher scale factors τ (around 15 to 100), the entropies $H[Y_\tau^+]$ and $H[Y_\tau^-]$ are almost constant (see examples in figure 7(a)). Moreover, we note that the asymmetry index $\hat{A}(\tau)$ wanders around 0, in a way similar to the one observed for the Gaussian white noises (see figure 7(b)).

The behaviors for the entropies $H[Y_\tau^+]$ and $H[Y_\tau^-]$ of positive and negative increments and for the asymmetry index $\hat{A}(\tau)$ of LDF signals (*peripheral* CVS) are different from the ones observed for HRV data (*central* CVS). By studying the time reversibility/irreversibility of central cardiovascular data (HRV signals) from healthy subjects, other authors have shown that entropies for positive and negative increments have a monotonic behavior for scale factors τ lower than 20 (in Costa *et al* (2005), τ varied from 1 to 20). From a qualitative point of view, the evolution of entropies $H[Y_\tau^+]$ and $H[Y_\tau^-]$ for positive and negative increments for LDF signals (peripheral CVS) presents a marked contrast pattern compared to the one of HRV data (central CVS). We find a nonmonotonic evolution of the entropies $H[Y_\tau^+]$ and $H[Y_\tau^-]$

with scale factor τ for the LDF signals. For HRV signals from healthy subjects, the evolution observed for the entropies $H[Y_\tau^+]$ and $H[Y_\tau^-]$ is monotonic with two trends: a light increasing trend for scale factors τ going from 1 to around 15 and a nearly constant value for scale factors τ going from around 15 to 100. Furthermore, the entropies $H[Y_\tau^+]$ and $H[Y_\tau^-]$ of LDF_R_{ECG} signals present patterns that are different from the one of LDF signals; two trends are noted for LDF_R_{ECG} signals: an increasing trend and then a decreasing one.

From a quantitative point of view, we note that the oscillations visible on the entropy $H[Y_\tau^+]$ for the positive increments Y_τ^+ and on the entropy $H[Y_\tau^-]$ for the negative increments Y_τ^- for LDF signals have a period equal to the one of the cardiac activity for each subject. These first results on the analysis of time reversibility/irreversibility for LDF data lead to new information on the properties of the microvascular perfusion time series. Moreover, these oscillations with a period of the cardiac activity are not visible on the entropy $H[Y_\tau^+]$ nor on the entropy $H[Y_\tau^-]$ of LDF_R_{ECG} signals. The cardiac activity may therefore play a role in the time irreversibility properties of LDF signals. This complements the results found previously (see for example Buard *et al* 2010, Humeau *et al* 2010a, 2010b, 2009, 2007a).

5. Conclusion

We herein focused on the time irreversibility characterization method proposed by Costa *et al* (2005) to analyze LDF, LDF_R_{ECG} and HRV signals. A theoretical analysis of the characterization method has been proposed to better appreciate its capabilities, behaviors and limitations. We thus studied analytically the behavior of the approach on several kinds of random signal models of known temporal constitution, so as to serve as references. Our results show that white fluctuations are always characterized as time reversible by the irreversibility indices $A(\tau)$ and $A'(\tau)$, as expected. Moreover, for Gaussian stationary colored fluctuations, we show that $A(\tau)$ and $A'(\tau)$ vanish for any correlation structure $\rho(\tau)$, thus characterizing Gaussian stationary colored fluctuations as reversible, as expected again. Moreover, we have shown that stationary white fluctuations with a multiplicative modulation are generally characterized as irreversible signals by the irreversibility indices $A(\tau)$ and $A'(\tau)$ (that are generally non-zero). However, when the white noise has a symmetric even probability density, the stationary white fluctuations with multiplicative modulation are characterized as reversible signals by the indices $A(\tau)$ and $A'(\tau)$. For stationary white fluctuations with additive modulation, the two indices $A(\tau)$ and $A'(\tau)$ will generally be non-zero thus leading to a characterization of the signals as irreversible signals. Other quantitative indices of multiscale irreversibility have been proposed (Hou *et al* 2010, Alvarez-Ramirez *et al* 2009, Casali *et al* 2008, Porporato *et al* 2007) and could be analyzed too.

The irreversibility index introduced in Costa *et al* (2005) is related to the assumption that 'each transition (increase or decrease in heart rate) is independent and requires a specific amount of energy'. This way of approach provides a connection to motivate or interpret the irreversibility index in a thermodynamic or statistical physics framework. However, at the level of an observed signal, the index keeps an intrinsic significance as a measure of time asymmetry, even if the assumption of underlying independent energetic transitions is not validated. By constitution, the irreversibility indices in Costa *et al* (2005) and those tested here, based on the probability distributions for the positive and for the negative increments, have the ability to detect any asymmetry that could exist, statistically, between the increasing and decreasing temporal transitions in an observed signal. And this ability, conditioned by asymmetries in the probability densities, is preserved whether or not successive increments are statistically independent. Accordingly, the irreversibility indices can be usefully applied to observed signals, as we performed here, without necessary reference to underlying independent

energetic transitions, which may indeed be difficult to validate for complex signals from cardiovascular dynamics.

We have undertaken the first application to study the time reversibility/irreversibility properties of LDF and LDF_R_{ECG} data. We also have confronted the results with those found from HRV data (central CVS) recorded simultaneously to LDF signals. Our work reveals that LDF signals present entropies of positive and negative increments ($H[Y_\tau^+]$ and $H[Y_\tau^-]$, respectively) that have oscillations with a period matching the one of the cardiac activity. Moreover, our results show that these oscillations with a period of the cardiac activity are not visible on the entropy $H[Y_\tau^+]$ nor on the entropy $H[Y_\tau^-]$ of LDF_R_{ECG} signals, nor on the ones of HRV data. The cardiac activity may therefore play a dominant role in the time irreversibility properties of LDF signals. Our findings could be used to test future models for LDF signals.

References

Al-Tahami B A, Yvonne-Tee G B, Halim A S, Ismail A A and Rasool A H 2010 Reproducibility of laser Doppler fluximetry and the process of iontophoresis in assessing microvascular endothelial function using low current strength *Methods Find. Exp. Clin. Pharmacol.* **32** 181–5

Alvarez-Ramirez J, Rodriguez E and Echeverria J C 2009 A DFA approach for assessing asymmetric correlations *Physica* A **388** 2263–70

Bernjak A, Deitrick G A, Bauman W A, Stefanovska A and Tuckman J 2011 Basal sympathetic activity to the microcirculation in tetraplegic man revealed by wavelet transform of laser Doppler flowmetry *Microvasc. Res.* **81** 313–8

Binzoni T, Seelamantula C S and Van De Ville D 2010 A fast time-domain algorithm for the assessment of tissue blood flow in laser-Doppler flowmetry *Phys. Med. Biol.* **55** N383–94

Binzoni T, Leung T S and Van De Ville D 2009 The photo-electric current in laser-Doppler flowmetry by Monte Carlo simulations *Phys. Med. Biol.* **54** N303–18

Buard B, Mahe G, Chapeau-Blondeau F, Rousseau D, Abraham P and Humeau A 2010 Generalized fractal dimensions of laser Doppler flowmetry signals recorded from glabrous and nonglabrous skin *Med. Phys.* **37** 2827–36

Casali K R, Casali A G, Montano N, Irigoyen M C, Macagnan F, Guzzeti S and Porta A 2008 Multiple testing strategy for the detection of temporal irreversibility in stationary time series *Phys. Rev.* E **77** 066204

Costa M, Goldberger A L and Peng C K 2005 Broken asymmetry of the human heartbeat: loss of time irreversibility in aging and disease *Phys. Rev. Lett.* **95** 198102

Costa M D, Peng C K and Goldberger A L 2008 Multiscale analysis of heart rate dynamics: entropy and time irreversibility measures *Cardiovasc. Eng.* **8** 88–93

Cover T M and Thomas J A 1991 *Elements of Information Theory* (New York: Wiley)

Hou F, Zhuang J, Bian C, Tong T, Chen Y, Yin J, Qiu X and Ning X 2010 Analysis of heartbeat asymmetry based on multi-scale time irreversibility test *Physica* A **389** 754–60

Hoyer D *et al* 2012 Fetal development assessed by heart rate patterns-time scales of complex autonomic control *Comput. Biol. Med.* **42** 335–41

Humeau A, Buard B, Chapeau-Blondeau F, Rousseau D, Mahé G and Abraham P 2009 Multifractal analysis of central (electrocardiography) and peripheral (laser Doppler flowmetry) cardiovascular time series from healthy human subjects *Physiol. Meas.* **30** 617–29

Humeau A, Buard B, Mahé G, Chapeau-Blondeau F, Rousseau D and Abraham P 2010b Multifractal analysis of heart rate variability and laser Doppler flowmetry fluctuations: comparison of results from different numerical methods *Phys. Med. Biol.* **55** 6279–97

Humeau A, Buard B, Mahé G, Rousseau D, Chapeau-Blondeau F and Abraham P 2010a Multiscale entropy of laser Doppler flowmetry signals in healthy human subjects *Med. Phys.* **37** 6142–6

Humeau A, Chapeau-Blondeau F, Rousseau D, Tartas M, Fromy B and Abraham P 2007a Multifractality in the peripheral cardiovascular system from pointwise Hölder exponents of laser Doppler flowmetry signals *Biophys. J.* **93** L59–61

Humeau A, Steenbergen W, Nilsson H and Stromberg T 2007b Laser Doppler perfusion monitoring and imaging: novel approaches *Med. Biol. Eng. Comput.* **45** 421–35

Ivanov P C, Amaral L A, Goldberger A L, Havlin S, Rosenblum M G, Struzik Z R and Stanley H E 1999 Multifractality in human heartbeat dynamics *Nature* **399** 461–5

Lotric M B, Stefanovska A, Stajer D and Urbancic-Rovan V 2000 Spectral components of heart rate variability determined by wavelet analysis *Physiol. Meas.* **21** 441–57

O'Doherty J, McNamara P, Clancy N T, Enfield J G and Leahy M J 2009 Comparison of instruments for investigation of microcirculatory blood flow and red blood cell concentration *J. Biomed. Opt.* **14** 034025

Okano K, Tsuruta Y, Yamashita T, Echida Y, Kabaya T and Nitta K 2010 Cardiovascular autonomic neuropathy studied by a laser-Doppler blood flowmeter in hemodialysis patients *Intern. Med.* **49** 2669–75

Papoulis A 1991 *Probability, Random Variables, and Stochastic Processes* (New York: McGraw-Hill)

Porporato A, Rigby J R and Daly E 2007 Irreversibility and fluctuation theorem in stationary time series *Phys. Rev. Lett.* **98** 094101

Signorini M G, Ferrario M, Cerutti S and Magenes G 2011 Advances in monitoring cardiovascular signals: contribution of nonlinear signal processing *Conf. Proc. IEEE Eng. Med. Biol. Soc.* vol 2011, pp 6568–71

Tew G A, Klonizakis M, Moss J, Ruddock A D, Saxton J M and Hodges G J 2011 Reproducibility of cutaneous thermal hyperaemia assessed by laser Doppler flowmetry in young and older adults *Microvasc. Res.* **81** 177–82

Wojtkiewicz S, Liebert A, Rix H and Maniewski R 2011 Evaluation of algorithms for microperfusion assessment by fast simulations of laser Doppler power spectral density *Phys. Med. Biol.* **56** 7709–23